




Climate change and water resources in arid regions: uncertainty of the baseline time period

Ruqayah Mohammed^{1,2} · Miklas Scholz^{2,3,4} 

Received: 24 August 2017 / Accepted: 11 October 2018
© The Author(s) 2018

Abstract

Recent climate change studies have given a lot of attention to the uncertainty that stems from general circulation models (GCM), greenhouse gas emission scenarios, hydrological models and downscaling approaches. Yet, the uncertainty that stems from the selection of the baseline period has not been studied. Accordingly, the main research question is as follows: What would be the differences and/or the similarities in the evaluation of climate change impacts between the GCM and the delta perturbation scenarios using different baseline periods? This article addresses this issue through comparison of the results of two different baseline periods, investigating the uncertainties in evaluating climate change impact on the hydrological characteristics of arid regions. The Lower Zab River Basin (Northern Iraq) has been selected as a representative case study. The research outcomes show that the considered baseline periods suggest increases and decreases in the temperature and precipitation (P), respectively, over the 2020, 2050 and 2080 periods. The two climatic scenarios are likely to lead to similar reductions in the reservoir mean monthly flows, and subsequently, their maximum discharge is approximately identical. The predicted reduction in the inflow for the 2080–2099 time period fluctuates between 31 and 49% based on SRA1B and SRA2 scenarios, respectively. The delta perturbation scenario permits the sensitivity of the climatic models to be clearly determined compared to the GCM. The former allows for a wide variety of likely climate change scenarios at the regional level and are easier to generate and apply so that they could complement the latter.

Keywords Climate change uncertainty · Baseline time period · Streamflow prediction · Hydro-climatic parameter forecasting

1 Introduction

1.1 Background

The “reference climate” or “baseline” time period can be defined as a period of time from which the potential climate

change projections are estimated. The establishment of a baseline period is commonly required for climate change and anthropogenic intervention impact studies. The baseline time period is a key factor in such studies and should be selected and gathered at the beginning of a project so that the potential future impacts can be evaluated against the previous situation; therefore, it serves as a benchmark for project success. The selection of the baseline has often been governed by the availability of the required climate data in addition to the study purpose.

The earlier baseline periods are preferred over later ones (IPCC 2007) for many reasons; for example, later periods such as 1961 to 1990 are likely to have larger trends incorporated with climate data, in particular, the effects of sulphate aerosols over Europe and eastern USA (IPCC 2007). Accordingly, the best baseline period would be in the nineteenth century when human-induced impacts on global climate were insignificant. However, most impact studies aim to determine the influence of climate change with respect to the presence, and therefore, recent baseline periods are

✉ Miklas Scholz
miklas.scholz@tvr.lth.se

¹ Faculty of Engineering, The University of Babylon, Hillah, Iraq
² Civil Engineering Research Group, School of Computing, Science and Engineering, The University of Salford, Newton Building, Peel Park Campus, Salford, Greater Manchester M5 4WT, UK
³ Division of Water Resources Engineering, Department of Building and Environmental Technology, Faculty of Engineering, Lund University, P.O. Box 118, SE-221 00 Lund, Sweden
⁴ Department of Civil Engineering Science, School of Civil Engineering and the Built Environment, University of Johannesburg, Kingsway Campus, PO Box 524, Auckland Park, Johannesburg 2006, South Africa

preferred (Semenov and Stratonovitch 2010). Furthermore, different approaches have different baseline requirements; the adequacy of the observed baseline can only be evaluated based on the construction methods of a specific climatic scenario. To apply the delta perturbation (DP) scenarios, many researchers (Tigkas et al. 2012; Al-Faraj and Scholz 2014; Mohammed and Scholz 2017c) used, as a baseline time period, certain periods that represent normal climatic conditions rather than using the entire available datasets. For example, in order to develop preparedness strategies to address the consequences of climate change such as drought phenomena, Mohammed and Scholz (2017c) utilised the DP climate scenario. For the DP scenario application, they defined the normal climatic time period through calculating the RDI values based on the entire datasets. Then, they selected the time period during which the RDI values are close to zero, which then can be considered for climate change and simulation studies.

Moreover, for the assessment of the impact of anthropogenic interventions on surface runoff, the concept and the identification of the baseline or the “pre-anomaly” period is different. If the studied hydrological regime has witnessed a sudden change such as a dam construction, then the Indicator of the Hydrological Alteration (IHA) can be applied to test how the flow system has changed through calculating the parameters for two time periods (before and after the alteration). However, if the flow system has experienced long-term human modifications, IHA can be used to evaluate changing trends. Additionally, in order to determine the artificial critical change points, many statistical (e.g. non-parametric analysis) and graphical (double mass curves, single mass curves and flow duration curves) methods are often used (Cheng et al. 2016; Mao et al. 2015; Mohammed et al. 2017a). In order to quantify both climate change and anthropogenic intervention impacts on the streamflow, Mohammed et al. (2017a) applied multi-regression, hydrologic model and hydrologic sensitivity simulation assessments. They used Pettitt, P-runoff double cumulative curve (PR-DCC) and Mann-Kendall techniques for the change points and significant trend assessments. The long-term runoff series from 1979 to 2013 was divided into baseline (1979–1997) and anthropogenic intervention (1998–2013) periods.

In general, for climate change impact quantification, the uncertainty that stems from GCM is considered to be the largest. Still, the uncertainty related to the baseline must be taken into consideration for better evaluation of the climate change impact. There is a need to calculate the effects of climate change on the hydrological characteristics of representative example case studies such as the Lower Zab River Basin, while exploring the uncertainties linked to the baseline time period using two time periods such as 1988–2000 and 1980–2010 in this case.

1.2 Aim, objectives and novelty

This study evaluated the climate change impacts on the flow within an example case study (Lower Zab River, Iraq), considering the uncertainty that stems from the baseline time period in addition to many other sources such as GCM, greenhouse gas emission scenarios, and DP procedures. This has been achieved by comparing the results of an ensemble of seven GCM methods under the Special Reports on Emission Scenarios SRA2 and SRA1B (Semenov and Stratonovitch 2010) using two different baseline time periods, with the perturbations of P (dP of 0–40%; 2% step) and potential evapotranspiration (PET) (dPET of 0–30%; 2% step). The comparison aims to explore how close these scenarios are and how different they are from each other in terms of their ability to simulate streamflow.

This research can be considered as an initial effort to answer the following open research question: What would be the differences and/or the similarities in the evaluation of climate change impact between the DP and the GCM scenarios using different baseline time periods? This is a remarkable question, as practically, all earlier climate change evaluation studies are generally based on only one baseline time period without taking into consideration the uncertainty that stems from using different baseline periods. Figure 1 shows the suggested procedure for the modelling approach of the evaluation of the potential influences of climate change on the water resource system.

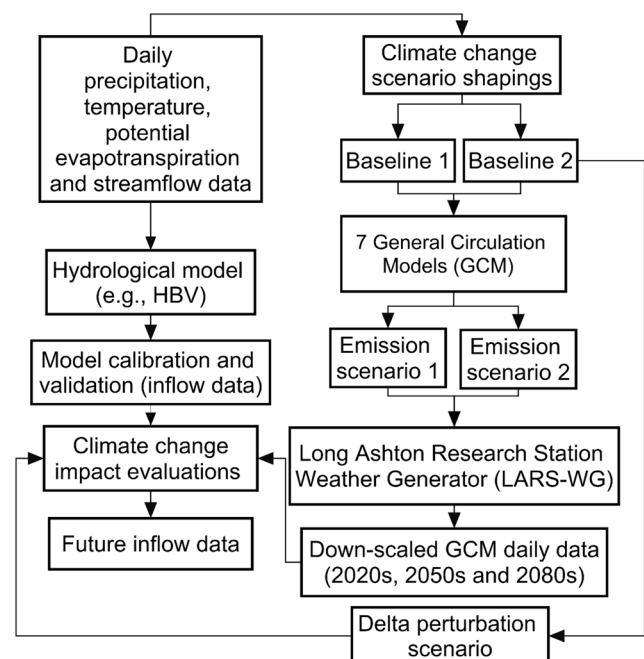


Fig. 1 The suggested new methodology for the assessment of the potential impacts of climate change on water resources systems. HBV Hydrologiska Byråns Vattenbalansavdelning hydrological model

Table 1 Name and locations of the meteorological stations that are distributed over the upper part of Lower Zab River Basin

Sit name	Longitude (°)	Latitude (°)	Elevation (m)
Sulymanya	45.45	35.53	885
Halabcha	45.94	35.44	651
Sachez	46.26	36.25	1536
Mahabad	45.70	36.75	1356
Salahddin	44.20	36.38	1088
Soran	44.63	36.87	1132

The main objectives are to (1) investigate the relevance of LARS-WG5.5 (Semenov and Stratonovitch 2010) for downscaling weather data at the LZRB and (2) to estimate the future variation and the uncertainties in the prediction of surface inflow to the basin storage system that could stem from: (a) climate change scenarios, which are GCM and DP; (b) emission scenarios SRA2 and SRA1B; and (c) the baseline time periods 1988–2000 and 1980–2010. The SRA2 and SRA1B scenarios define a locally oriented economy leading to a heterogeneous world and a balanced technology and fossil fuel-oriented rapid growth, respectively. The outcomes of this study will be beneficial to investigate the effect of climate

change on the inflow to the basin storage system in arid climatic condition.

2 Materials and methods

2.1 Data collection

The following data have been collected: (1) Daily weather data such as P as well as maximum and minimum air temperature from six gauging stations were obtained for the water year range between 1979/80 and 2012/13. The weather gauging stations are distributed over the upper part sub-basin of the study area with elevations varying from 651 to 1536 m (Table 1 and Fig. 2). (2) Daily flow data at Dokan hydrological station (latitude 35° 53' 00" N; Longitude 44° 58' 00" E) are available for the water year range between 1931/32 and 2013/14. The catchment area for the upper part of the LZRB is about 12,096 km². The data were received from the Ministry of Agriculture and Water Resources for the Kurdistan Province of Iraq. (3) Geospatial data: Iraqi boundaries and the LZRB shape files have been downloaded from the Global Administrative Areas (GADM, Global Administrative Areas Database, 2012) and the Global and Land Cover

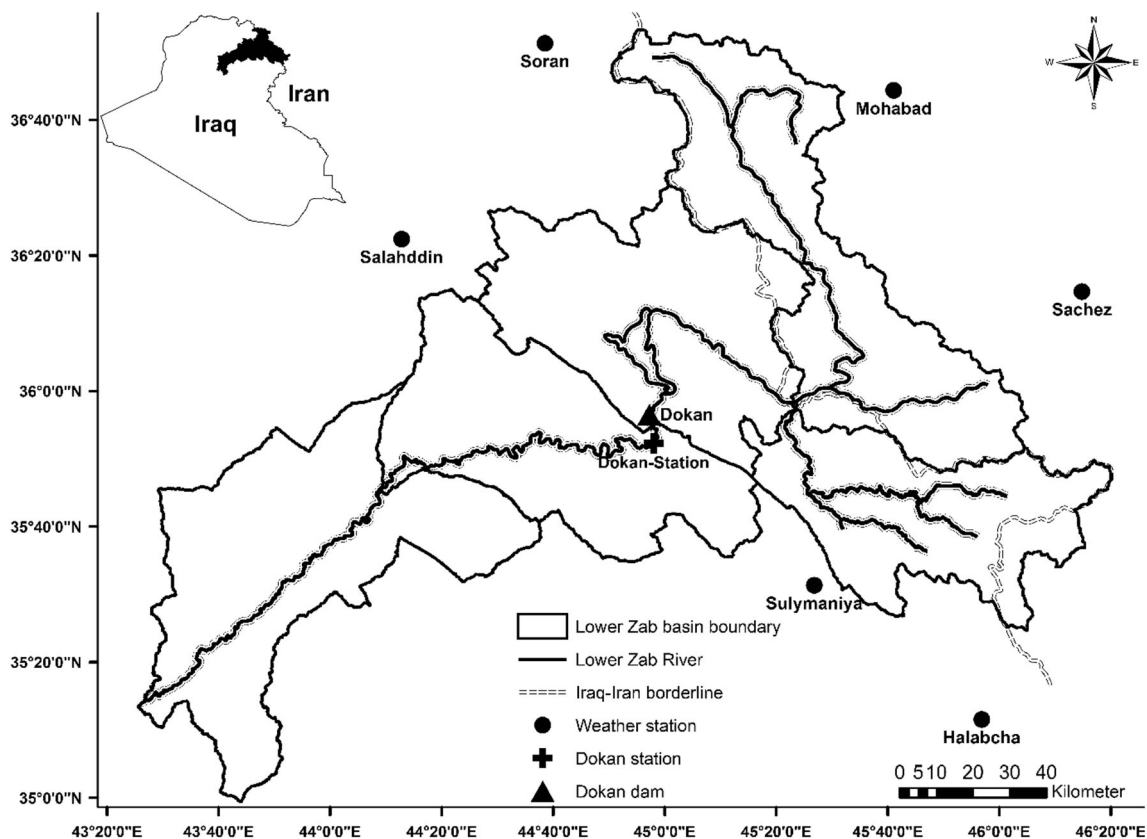


Fig. 2 Locations of the representative basin including the locations of the hydro-climatic stations

Table 2 Global climate models (GCM) from the Intergovernmental Panel on Climate Change (IPCC) fourth assessment report (AR4) integrated into the Long Ashton Research Station Weather Generator (LARS-WG5). T₁, 2011–2030; T₂, 2046–2065; T₃, 2081–2100 (adopted from Semenov and Stratonovitch (2010))

Global climate model	Model acronym	Grid (°)	Time period	Country	Source
Special Report on Emissions Scenarios SRA1B					
CGCM33.1 (T ₄₇) ^a	CGMR	2.8 × 2.8	T ₁ , T ₂ , T ₃	Canada	McFarlane et al. (1992)
Special Report on Emissions Scenarios SRA1B, SRB1					
CSIRO-MK3.0 ^b	CSMK3	1.9 × 1.9	T ₁ , T ₂ , T ₃	Australia	Gordon et al. (2002) and CSMD, Climate System Modeling Division (2005)
FGOALS-g1.0 ^c	FGOALS	2.8 × 2.8	T ₁ , T ₂ , T ₃	China	Wang et al. (2004)
MRI-CGCM2.3.2 ^d	MIHR	2.8 × 2.8	T ₁ , T ₂ , T ₃	Japan	K-1 Model Developers (2004)
BCM2.0 ^e	BCM2	1.9 × 1.9	T ₁ , T ₂ , T ₃	Norway	Déqué et al. (1994)
GISS-AOM ^f	GIAOM	3 × 4	T ₁ , T ₂ , T ₃	USA	Russell et al. (1995)
PCM ^g	NCPCM	2.8 × 2.8	T ₁ , T ₂	USA	Kiehl et al. (1998) and Kiehl and Gent (2004)
Special Reports on Emissions Scenarios SRA1B and SRA2					
HadGEM1 ^h	HADGEM	1.3 × 1.9	T ₁ , T ₂ , T ₃	UK	Martin et al. (2006) and Ringer et al. (2006)
CNRM-CM3 ⁱ	CNCM3	1.9 × 1.9	T ₁ , T ₂ , T ₃	France	Déqué et al. (1994)
Special Reports on Emission Scenarios SRA1B, SRA2 and SRB1					
GFDL-CM2.1 ^j	GFCM21	2.0 × 2.5	T ₁ , T ₂ , T ₃	USA	GFDL-GAMDT, GFDL Global Atmospheric Model Development Team (2004)
HadCM3 ^k	HADCM3	2.5 × 3.75	T ₁ , T ₂ , T ₃	UK	Gordon et al. (2000) and Pope et al. (2000)
INM-CM3.0 ^l	INCM3	4 × 5	T ₁ , T ₂ , T ₃	Russia	Galin et al. (2003)
IPSL-CM4 ^m	IPCM4	2.5 × 3.75	T ₁ , T ₂ , T ₃	France	Hourdin et al. (2006)
ECHAM5-OM ⁿ	MPEH5	1.9 × 1.9	T ₁ , T ₂ , T ₃	Germany	Roeckner et al. (1996)
CCSM3 ^o	NCCCS	1.4 × 1.4	T ₁ , T ₂ , T ₃	USA	Collins et al. (2004)

^a Canadian Centre for Climate Modelling and Analysis; ^b Commonwealth Scientific and Industrial Research Organisation; ^c Institute of Atmospheric Physics; ^d National Institute for Environmental Studies; ^e Bjerknes Centre for Climate Research; ^f Goddard Institute for Space Studies; ^g National Centre for Atmospheric; ^h UK Meteorological Office; ⁱ Centre National de Recherches Meteorologiques; ^j Geophysical Fluid Dynamics Lab; ^k UK Meteorological Office; ^l Institute for Numerical Mathematics; ^m Institute Pierre Simon Laplace; ⁿ Max-Planck Institute for Meteorology; ^o National Centre for Atmospheric Science

Table 3 Carbon dioxide (CO₂) concentrations for selected climate scenarios specified in the Special Report on Emissions Scenarios (adopted from Semenov and Stratonovitch (2010))

Scenario	Key assumptions	CO ₂ concentration (parts per million)		
		T ₁	T ₂	T ₃
B ₁ : the sustainable world	Quick alteration in economic organisations; dematerialisation comprising developed equity and ecological concern; global concern regarding ecological and social sustainability; more effort in introducing clean technologies; world population extends to 7 billion by 2100	410	492	538
B ₂ : the world of technological inequalities	A heterogeneous society emphasising local solutions to economic, social and environmental sustainability rather than global solutions; human welfare, equality and environmental protection all have high priority.	406	486	581
A ₁ B: the rich world	Characterised by very rapid economic growth (3% a year), low population growth (0.27% a year) and rapid introduction of new and more efficient technologies; globally, there is economic and cultural convergence and capacity building; substantial reduction in regional differences in per capita income.	418	541	674
A ₂ : the separated world	Cultural characteristics distinct the diverse areas, making the world more heterogeneous and international cooperation less likely; high “family values”, strong local traditions and high population growth (0.83% a year); less focus on economic development (1.65% a year) and material wealth.	414	545	754

Facility (GLCF, Global and Land Cover Facility, 2015) databases, respectively.

2.2 Data analysis

The following analysis have been performed: (1) For the hydro-climatic gauging station location projections, Theissen network, basin boundary and streamflow delineations, ArcGIS 10.3 software has been applied. (2) For the analysis of the daily hydro-climatic datasets such as trend, monthly and annual amounts, modifications and filling of data gaps were estimated by the Statistical Program for Social Sciences program (SPSS) 23 (ITS 2016). (3) To transform Microsoft Excel software charts to images with specific dimensions and resolutions, Daniel's XL Toolbox (<http://daniel-s-xl-toolbox.software.informer.com/download>) was used; this is an open-source Add-In for Excel. (4) To run the HBV rainfall-runoff model, RS MINERVE2.5 has been used (<https://www.crealp.ch/down/rsm/install2/archives.html>). RS MINERVE is a free downloadable software for the simulation of free surface runoff flow formation and propagation (Foehn et al. 2016).

2.3 Representative study example

The proposed methodology was applied to the Lower (Lesser/Little) Zab River, which is considered one of the most important tributaries of the Tigris River stream. The Lower Zab River is situated in Erbeel Governorate. The watercourse network is located between latitudes 36° 50' N and 35° 20' N and longitudes 43° 25' E and 45° 50' E (Mohammed et al. 2017a) as shown in Fig. 2. Dokan is the most important dam that has been constructed on the Iraqi part of the shared basin. The dam is a multi-function arch dam with an extreme storage size of approximately 6.970 billion cubic meters (BCM), a top elevation of 116 m above the river bed (516 m) and a stretch of 360 m (Mohammed et al. 2017b).

The LZRB has been selected as an example basin for arid and semi-arid areas. The nature of the study is common to other shared river basins such as the Senegal, Volta and Rhine, where challenges of shared sustainable water resource use are anticipated to exacerbate under the collective impact of climate change (Mohammed and Scholz 2017a, b). The upstream and downstream developments vary widely. This suggests a varied range of uncertainties in climate change impacts on water resources availability.

2.4 Downscaling model

The Long Ashton Research Station Weather Generator (LARS-WG5.5) has been used to predict meteorological variables at a single site under the current and future climate conditions. The process of artificial climate generation is divided into three stages (Semenov and Stratonovitch 2010):

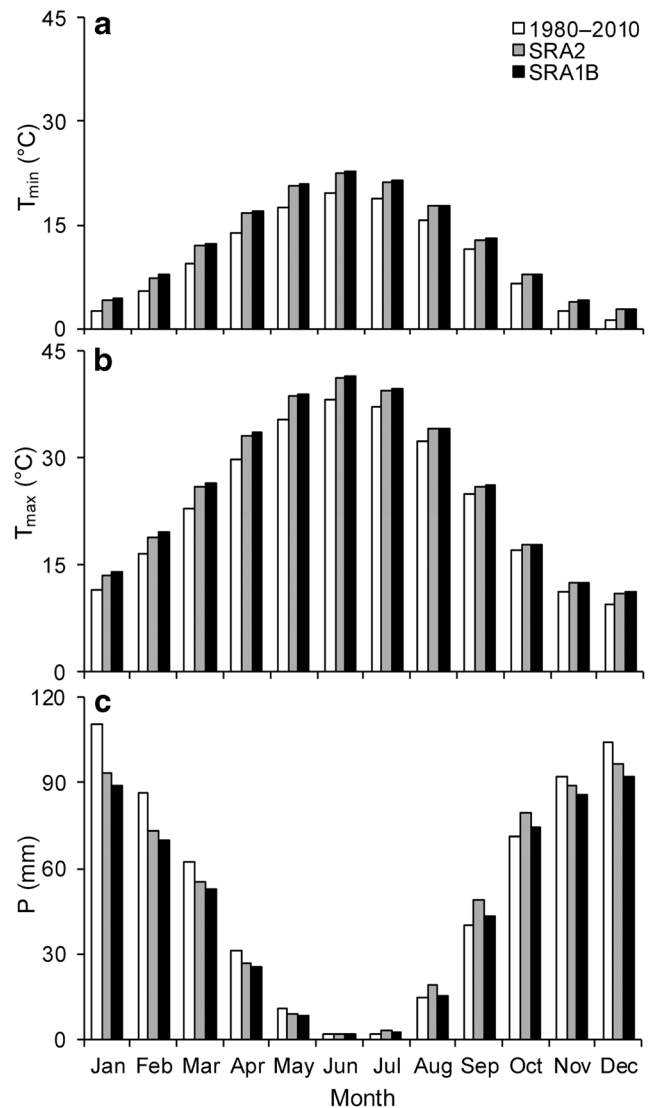
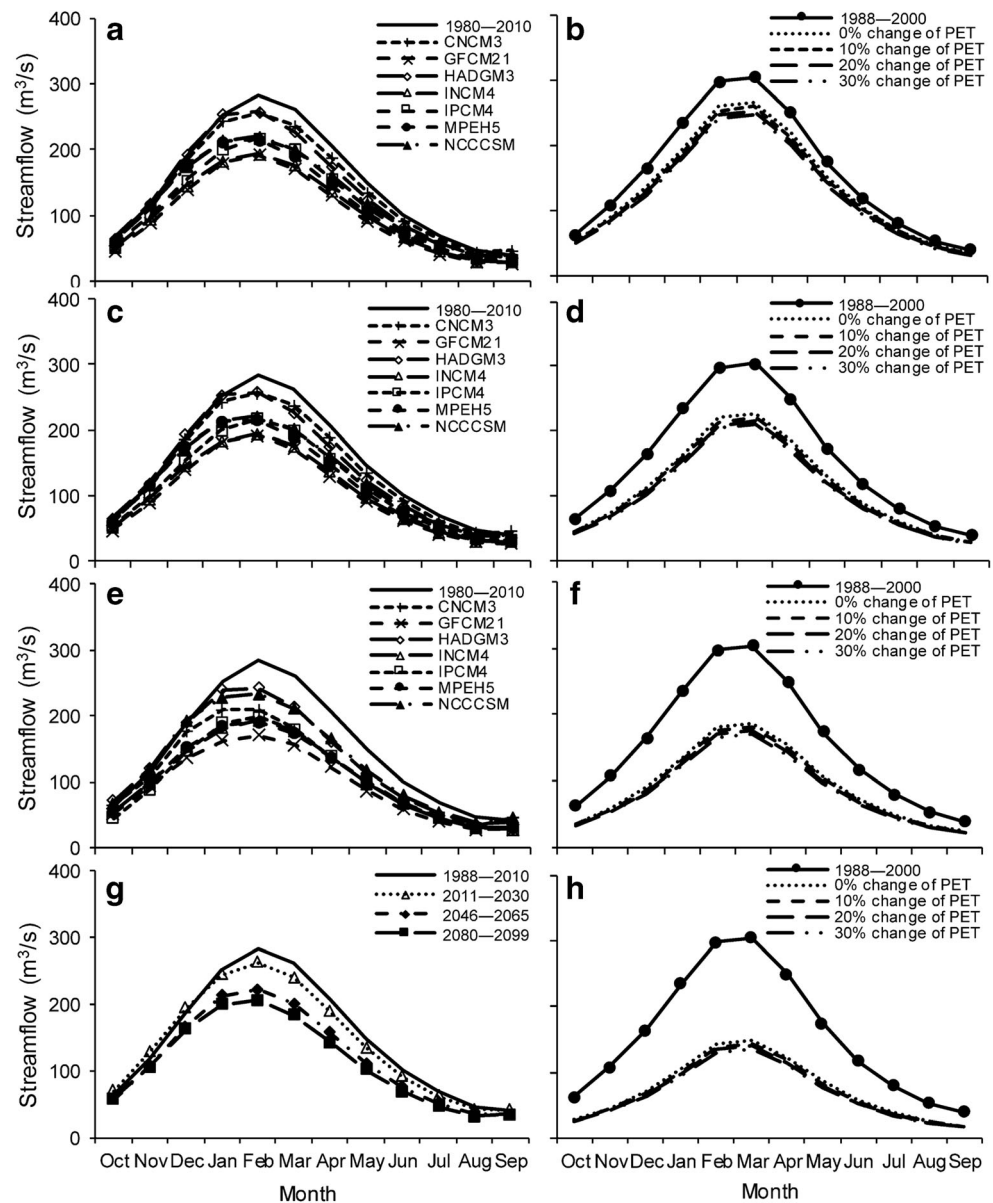


Fig. 3 Mean monthly **a** minimum temperature (T_{\min}); **b** maximum temperature (T_{\max}); and **c** precipitation (P) for the 2046–2065 period. Downscaling from seven ensemble general circulation models (GCM) under two emission scenarios, which are the Special Report on Emissions Scenarios SRA2 and SRA1B, took place

- (1) Site analysis: this function is used for the model calibration by analysis of the statistical properties of the observed weather variables. The statistical properties are saved in two files;
- (2) The Q_{Test} function is used for model validation during which the statistical properties of the observed and the generated weather variables are used to examine if there are any statistically significant variations; and
- (3) The generator: this function is used for the generation of artificial weather variables. The files resulting from the calibration of the model are used to produce synthetic weather variables having the same statistical properties as the observed ones, but are different on a day-to-day basis. The climate scenarios in this research are based on

Fig. 4 Changes in the timing and the magnitude of the predicted mean monthly inflow to the Dokan reservoir under the general circulation model (GCM) scenarios (left figures; Fig. 4a–g) based on the Special Report on Emissions Scenarios SRA1B: **a** 2011–2030; **c** 2046–2065; and **e** 2080–2099; time horizon, and **g** comparison of the three future time horizon, compared to baseline 1 (1980–2010) values; and delta perturbation scenarios (right figures; Fig. 4b–h): **b** 10% reduction in precipitation (P); **d** 20% reduction in P; **f** 30% reduction in P; and **h** 40% reduction in P, compared to the baseline 2 (1988–2000) values. CNCM3, Centre National de Recherches, France; GFCM21, Geophysical Fluid Dynamics Lab, USA; HADGM3, UK Meteorological Office; INCM3, Institute for Numerical Mathematics, Russia; IPCM4, Institute Pierre Simon Laplace, France; MPEH5, Max-Planck Institute for Meteorology, Germany; and NCCCSM, National Centre for Atmospheric Science, USA



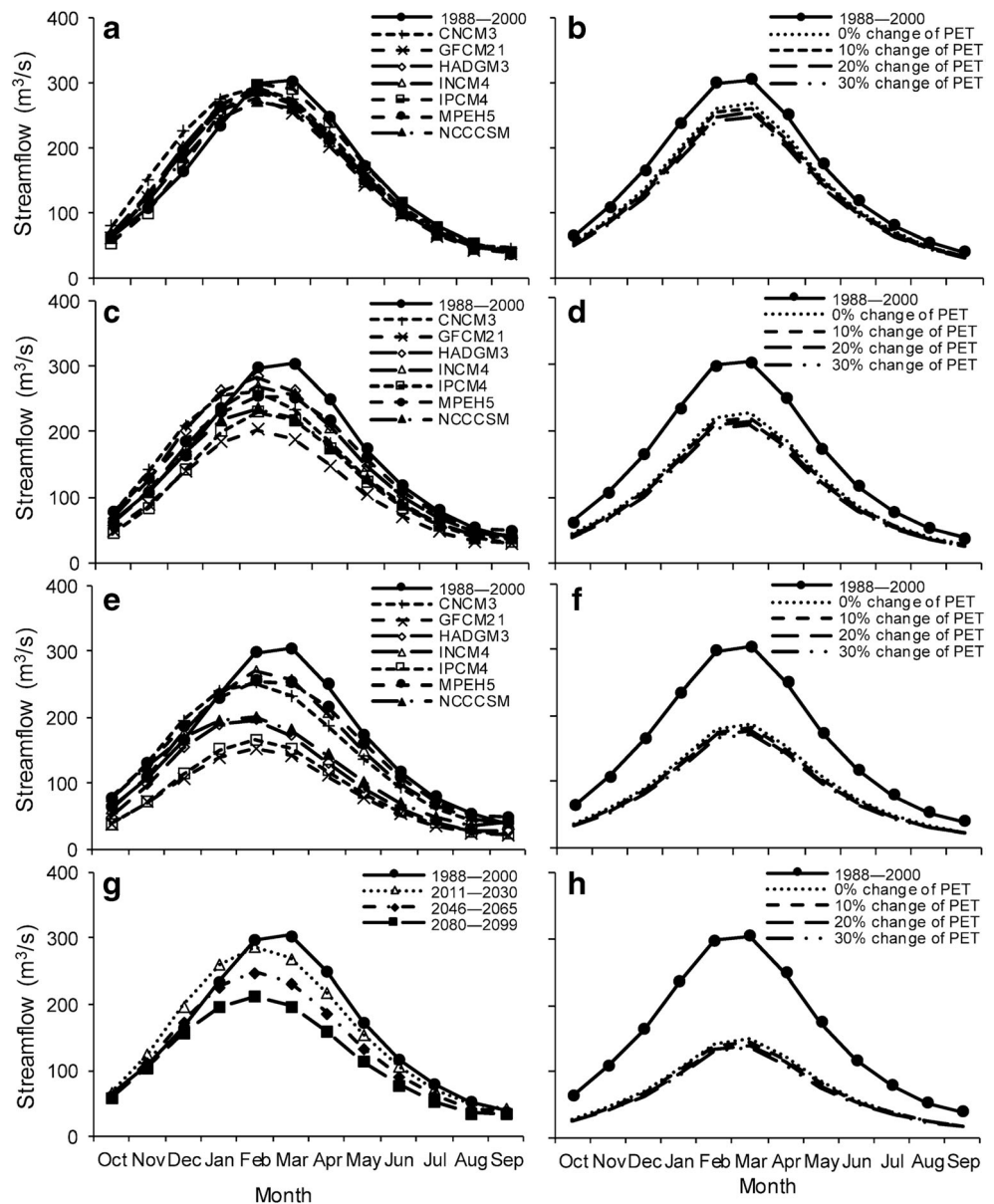
the SRA2 and SRA1B emission scenarios modelled by seven GCM ensembles (Tables 2 and 3) and simulated by applying LARS-WG5.5 for the 2011–2030 (near future), 2046–2065 (medium future) and 2080–2099 (far future) time horizons in addition to two baseline time periods. The first time period (1988–2000) represents normal climate. The RDI values are close to zero. This period can be considered for climate change and simulation studies. The water years between 1980 and 2010 comprise the second time period, which has been selected to determine the influence of climate change with respect to the presence.

The AR5 report brings decision-makers up-to-date on the state of climate science. Since it is released in stages, it is the

most complete evaluation of existing climate change studies and gives a baseline for understanding and future actions. Moreover, among the highlights of the AR5 report, the conclusion that much of the warming over the past five decades resulted from anthropogenic intervention is now “extremely likely” (“very likely” in the AR4 report). Predictions of the future rise in sea level have been considerably improved, because of the enhancement in the understanding of the ice sheet movements in temperate weather. Additionally, the Arctic Ocean is now projected to be ice-free during the summer by the mid-century (end-of-century in AR4 report) under a high greenhouse gas emission scenario.

However, there are no remarkable changes in the AR5 report, which are linked to previous models released as part of the AR4 report and earlier assessment reports. Nevertheless, there is a noticeable rise in the volume of data and a steady

Fig. 5 Changes in the timing and the magnitude of the predicted mean monthly inflow to the Dokan reservoir under the general circulation model (GCM) scenarios (left figures; Fig. 5a–g) based on the Special Report on Emissions Scenarios SRA2: (a) 2011–2030; (c) 2046–2065; and (e) 2080–2099 time horizons, and (g) comparison of the three future time horizons to the baseline (1988–2000) values; and delta perturbation scenarios (right figures; Figs. 5b–h): (b) 10% reduction in precipitation (P); (d) 20% reduction in P; (f) 30% reduction in P; and (h) 40% reduction in P compared to the baseline (1988–2000) values. CNCM3, Centre National de Recherches, France; GFCM21, Geophysical Fluid Dynamics Lab, USA; HADGM3, UK Meteorological Office; INCM3, Institute for Numerical Mathematics, Russia; IPCM4, Institute Pierre Simon Laplace, France; MPEH5, Max-Planck Institute for Meteorology, Germany; and NCCCSM, National Centre for Atmospheric Science, USA



increase in the number of modelling research groups providing their technical perspectives to the modelling community. Accordingly, this research utilised LARS5.5 for downscaling weather data over the study area based on the reasoning of the IPCC AR4 report.

3 Results and discussion

3.1 Weather parameters and reservoir inflow

Thirty hydrological years were utilised for the calibration and validation of the LARS-WG5.5 model. To assess the model performance, some graphical comparisons and statistical analysis were applied. For the analysis of the

equivalence of the wet/dry series periodic distributions, daily rainfall distributions as well as daily minimum and maximum temperature distributions, the Kolmogorov-Smirnov (K-S) method (Chen et al. 2013) was applied. The p value was used as an indicator, if there is a significant change between the simulated and the observed climatic parameters. A high K-S value and a very low p value mean that the simulated climate is unlikely to be identical to the observed one (Semenov et al. 2013). The obtained results from the LARS-WG model proved that the model performs well in producing weather data for most stations. Accordingly, the model can be applied to predict daily meteorological parameters for the stations for the time periods 2011–2030, 2046–2065 and 2080–2099, subject to seven ensembles of GCM as well as the SRA2 and SRA1B scenarios.

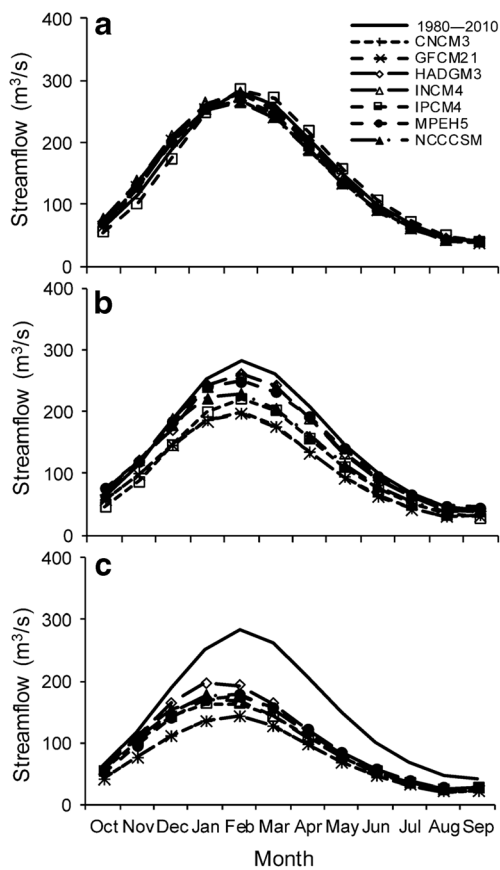


Fig. 6 Changes in the timing and the magnitude of the predicted mean monthly inflow to the Dokan reservoir under the general circulation model (GCM) scenarios based on the Special Report on Emissions Scenarios SRA2: **a** 2011–2030; **b** 2046–2065; and **c** 2080–2099 time horizons compared to the baseline (1980–2010) values. CNCM3, Centre National de Recherches, France; GFCM21, Geophysical Fluid Dynamics Lab, USA; HADCM3, UK Meteorological Office; INCM3, Institute for Numerical Mathematics, Russia; IPCM4, Institute Pierre Simon Laplace, France; MPEH5, Max-Planck Institute for Meteorology, Germany; and NCCCS, National Centre for Atmospheric Science, USA

Figure 3 reveals the mean values of the weather parameters resulting from seven ensembles of GCM under the SRA2 and SRA1B emission scenarios for the 2046–2065 future time period. Compared to the 1980–2010 baseline period, there is a rising trend in T_{\min} and T_{\max} and a declining trend in P values. The corresponding monthly values vary from month to month. The maximum increases in the predicted variables were 3.02 and 3.33 °C, 3.17 and 3.70 °C and 17.33 and 21.93 mm for the two considered emission scenarios, respectively. Figures 4 and 5 show the timing and the magnitude of the streamflow hydrographs simulated with meteorological data predicted by seven GCM that were downscaled using LARS-WG5.5 and DP for climate change scenarios, respectively. In order to avoid any bias resulting from the hydrological simulation process, the streamflow for the baseline periods, whether it is baseline 1 (1980–2010) or baseline 2 (1988–2000), is represented by modelled flow. The results

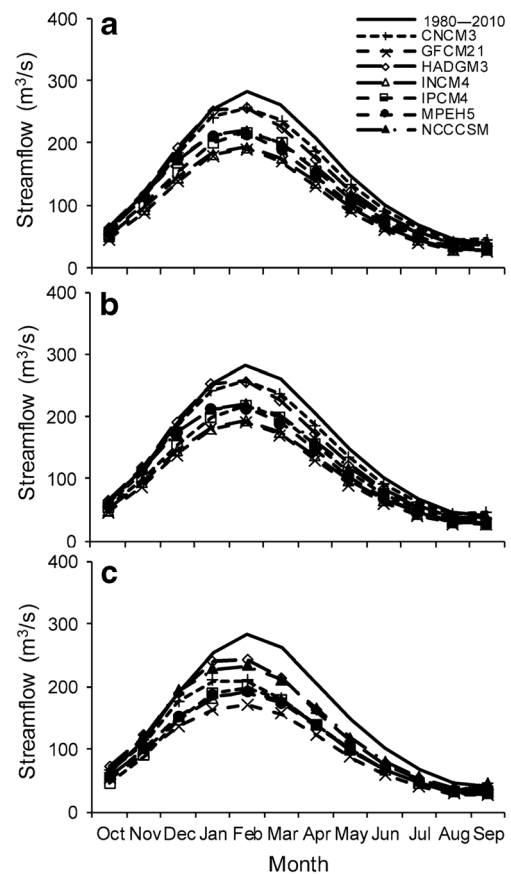


Fig. 7 Changes in the timing and the magnitude of the predicted mean monthly inflow to the Dokan reservoir under the general circulation model (GCM) scenarios based on the Special Report on Emissions Scenarios SRA1B: **a** 2011–2030; **b** 2046–2065; and **c** 2080–2099 time horizons compared to the baseline (1980–2010) values. CNCM3, Centre National de Recherches, France; GFCM21, Geophysical Fluid Dynamics Lab, USA; HADCM3, UK Meteorological Office; INCM3, Institute for Numerical Mathematics, Russia; IPCM4, Institute Pierre Simon Laplace, France; MPEH5, Max-Planck Institute for Meteorology, Germany; and NCCCS, National Centre for Atmospheric Science, USA

indicate how climate change might cause a reduction in both timing and magnitude of the inflow hydrograph to the reservoir. Both the GCM and DP climatic scenarios predict nearly the same declines in the mean monthly flows, and subsequently, their peak points are approximately the same. Figure 4 shows a declining trend in the inflow peaks fluctuating from 3% (INCM4) to 21% (GFCM21) as shown in Fig. 4a, 9% (CNCM3) to 39% (GFCM21) as presented in Fig. 4c and 21% (NCCCSM) to 42% (GFCM21) as highlighted in Fig. 4e for the three future time periods, respectively.

Further, to compare the results of the GCM and DP scenarios, the following has been highlighted: Firstly, based on the SRA1B emission scenario, Fig. 4g shows that the inflow to the reservoir is expected to decrease by about 10% for the 2011–2030 horizon, which is identical to the anticipated reservoir inflow applying DP (10% P decrease and 0% PET) as Fig. 4b shows. Figure 4g highlights that the equivalent

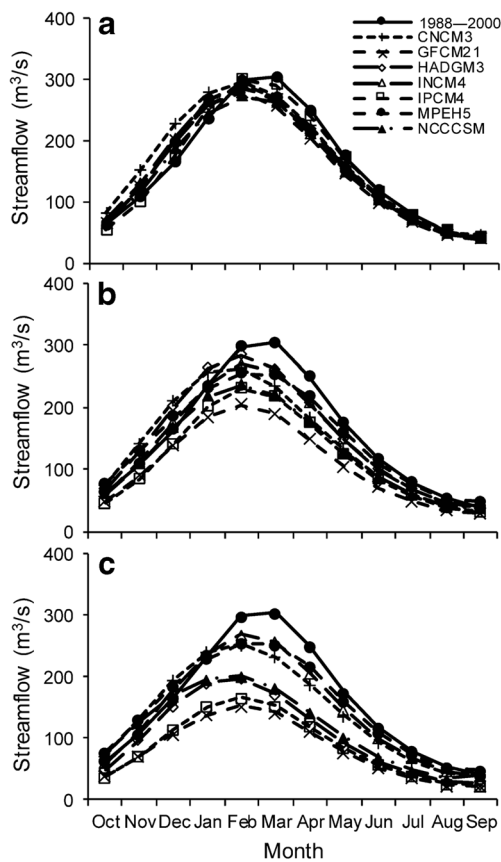


Fig. 8 Changes in the timing and the magnitude of the predicted mean monthly inflow to the Dokan reservoir under the general circulation model (GCM) scenarios based on the Special Report on Emissions Scenarios SRA2: **a** 2011–2030; **b** 2046–2065; and **c** 2080–2099 time horizons compared to the baseline (1988–2000) values. CNCM3, Centre National de Recherches, France; GFCM21, Geophysical Fluid Dynamics Lab, USA; HADCM3, UK Meteorological Office; INCM3, Institute for Numerical Mathematics, Russia; IPCM4, Institute Pierre Simon Laplace, France; MPEH5, Max-Planck Institute for Meteorology, Germany; and NCCCS, National Centre for Atmospheric Science, USA

decrease for the time period 2046–2065 is expected to be approximately 25%, which is identical to the predicted decrease in streamflow applying DP (20% decrease in P and 0% PET) as indicated by Fig. 4d. However, the predicted decline in the reservoir inflow for the 2080–2099 horizon is almost 32% (Fig. 4g), which is identical to the hydrograph that is shown in Fig. 4b (10% P reduction and 30% increase in PET).

Secondly, and based on the SRA2, all GCM show decreases in peak values ranging between 4% (IPCM4) and 19% (GFCM21) as presented in Fig. 5a, 16% (HADGM3) to 40% (GFCM21) as Fig. 5c shows, and 13% (MPEH5) to 56% (GFCM21) as highlighted in Fig. 5e for the three time horizons in this order. It is expected that the reservoir inflow will decline by approximately 13% by the 2020 horizon, Fig. 5g shows that the reservoir inflow is equal to the anticipated inflow by DP (10% P decrease and 0% PET) as Fig. 5b

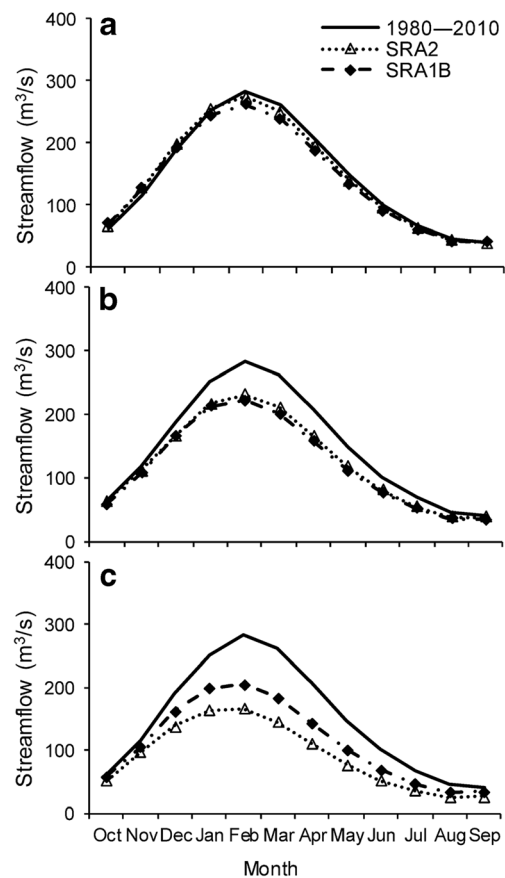


Fig. 9 Changes in the timing and magnitude of the predicted mean monthly inflow to the Dokan reservoir under the general circulation model (GCM) scenarios based on the Special Reports on Emissions Scenarios SRA2 and SRA1B: **a** 2011–2030; **b** 2046–2065; and **c** 2080–2099 time horizons compared to the baseline (1980–2010) values

demonstrates. The equivalent decrease for the time period 2046–2065 is expected to be nearly 25%, which is identical to the predicted decrease in streamflow by DP (20% decrease in P and 0% PET) as indicated in Fig. 5d. However, the predicted decline in the reservoir inflow for the 2080–2099 horizon is almost 36% (Fig. 5g), which is identical to the hydrograph shown by Fig. 5f (30% P reduction and 0% increase in PET). Moreover, Figs. 4 and 5a, c, e, and g confirm that maximum discharges were observed earlier than for the reference period (1988–2000), since the lag was about 8 days for nearly all the future time periods. Whereas there was not any variation in the time to maximum flowrate that was anticipated by the DP scenario, as indicated by Figs. 4 and 5b–h.

3.2 Uncertainty of reservoir inflow

Figures 6 and 7 display the uncertainty related to the GCM scenarios for three time horizons based on the baseline 1980–2010 and two emission scenarios, respectively. Figure 6a shows that during the 2020 time horizon, the seven GCM predict the inflow similarly. However, there is an evident

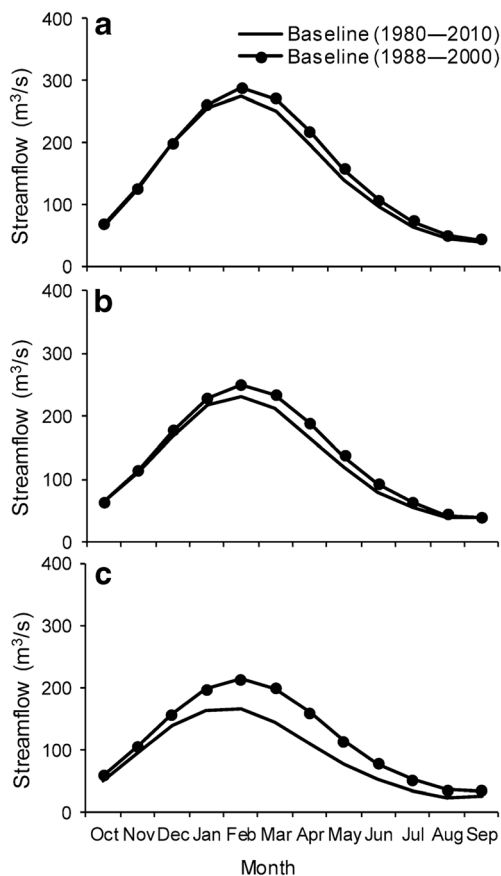


Fig. 10 Changes in the timing and magnitude of the predicted mean monthly inflow to the Dokan reservoir under the general circulation model (GCM) scenario under the Special Report on Emissions Scenarios SRA2: **a** 2011–2030; **b** 2046–2065; and **c** 2080–2099 time horizons for the two baseline time periods 1980–2010 and 1988–2000

uncertainty in the inflow prediction using different GCM for 2046–2065 and 2080–2099 (Fig. 6b, c), and all the time periods (Figs. 7a–c and 8a–c), respectively. This uncertainty stems from both GCM and emission scenarios.

Furthermore, the simulation results discussed how the SRA2 and SRA1B emission scenarios predict approximately the same decreases in the mean monthly flows, and consequently, their peak values are almost the same, in particular for the 2011–2030 and 2046–2065 time periods (Fig. 9a, b). There is no great variation in the predicted values of the reservoir inflows for the 2020s and 2050s, since the two emission scenarios show decreases in peak values ranging between 6% (SRA2) and 10% (SRA1B) as shown in Fig. 9a, and between 21% (SRA2) and 25% (SRA1B) as indicated by Fig. 9b. However, there is a clear variation in the predicted inflow using the two considered emission scenarios for the 2080–2099 time period. The variation altered from 31% (SRA1B) to 49% (SRA2) as illustrated in Fig. 9c.

By the 2020 horizon, there will be a decrease of between 6 and 13% in the mean monthly basin runoff (Fig. 10a) based on the baseline time periods 1980–2010 and 1988–2000,

respectively, which is identical to the predicted values by DP (10% P reduction and 0% PET) as indicated by Fig. 5b. The corresponding decrease for the time horizon 2046–2065 will be between 21 and 25%, which is identical to the predicted decrease in streamflow by DP (20% reduction in P and 0% PET increase) as highlighted in Fig. 5d. However, the anticipated runoff decrease for the last time horizon is between 31 and 36% (Fig. 10c), which is identical to the value obtained via DP as highlighted by Fig. 10f, (30% P reduction and 0% PET increase). It is expected that the reservoir inflow peak point will decrease, and there is likely to be a noticeable change in the flow amount, which may lead to a considerable impact on water resources management of this example basin.

4 Conclusions and recommendations

In order to enhance adaptation strategies to climate change, this study proposed a simple and generic methodology. The following conclusions can be drawn:

- The downscaling model LARS-WG5.5 predicted meteorological data in arid and semi-arid areas well and should be applied for prediction of daily future values.
- There will be a likely increase of about 3.02 and 3.33 °C and 3.17 and 3.70 °C in T_{\min} and T_{\max} for the 2046–2065 time period and the two considered baselines, respectively. However, there may be a decreasing trend of nearly 17.33 and 21.93 mm in the corresponding P values and the relative variations will fluctuate monthly.
- Both 1988–2000 and 1980–2010 baseline time periods anticipated almost similar reductions in the average monthly inflow to the reservoir, and subsequently, their peak points are nearly the same. For example, the predicted reduction in the reservoir inflow for the 2080–2099 period was between 31 and 36%, which is equivalent to the assessment from the DP scenario (30% P decrease and 0% PET rise).
- The SRA2 and SRA1B scenarios forecast approximately the same reductions in the mean monthly reservoir inflows; accordingly, their maximum values are almost the same, in particular for the 2011–2030 and 2046–2065 time periods. The two emission scenarios show decreases in peak values ranging between 6% (SRA2) and 10% (SRA1B), 21% (SRA2) and 25% (SRA1B) and 31% (SRA1B) and 49% (SRA2) for the three future time periods, respectively.
- There will be a reduction in the average monthly reservoir inflow as a result of P reduction.

By considering as many climate change and emission scenarios as well as baseline time period as practically possible, the water resource policy makers can adapt to the expected

impacts of climate change efficiently. This study should be undertaken again for other areas and climate types using different baseline time periods, which should lead to a further generalisation of the study conclusions.

Acknowledgements The authors are thankful to the Ministry of Agriculture and Water Resources of the Kurdistan Province of Iraq for providing the necessary data required to undertake this study.

Funding information The Iraqi government has financed the research via a PhD scholarship for the first author via Babylon University.

Open Access This article is distributed under the terms of the Creative Commons Attribution 4.0 International License (<http://creativecommons.org/licenses/by/4.0/>), which permits unrestricted use, distribution, and reproduction in any medium, provided you give appropriate credit to the original author(s) and the source, provide a link to the Creative Commons license, and indicate if changes were made.

References

- Al-Faraj F, Scholz M (2014) Incorporation of the flow duration curve method within digital filtering algorithms to estimate the base flow contribution to total runoff. *Water Resour Manag* 28(15):5477–5489. <https://doi.org/10.1007/s11269-014-0816-7>
- Chen H, Guo J, Zhang Z, Xu CY (2013) Prediction of temperature and precipitation in Sudan and South Sudan by using LARS-WG in future. *Theor Appl Climatol* 113(3–4):363–375. <https://doi.org/10.1007/s00704-012-0793-9>
- Cheng Y, He H, Cheng N, He W (2016) The effects of climate and anthropogenic activity on hydrologic features in Yanhe River. *Adv Meteorol* 5297158:11–11. <https://doi.org/10.1155/2016/5297158>
- Collins WD, Hack JJ, Boville BA, Rasch PJ and others (2004) Description of the NCAR Community atmosphere model (CAM3.0). Technical note TN-464+STR, National Center for Atmospheric Research, Boulder, CO
- CSMD, Climate System Modeling Division (2005) An introduction to the first general operational climate model at the National Climate Center. *Advances in Climate System Modeling 1*, National Climate Center, China Meteorological Administration
- Déqué M, Dreveton C, Braun A, Cariolle D (1994) The ARPEGE/IFS atmosphere model: a contribution to the French community climate modeling. *Clim Dyn* 10(4):249–266
- Foehn A, García Hernández J, Roquier B, Paredes Arquiola J (2016) RS MINERVE – User’s manual v2.6. RS MINERVE Group, Switzerland
- GADM, Global Administrative Areas Database (2012) Boundaries without limits [Online] Available from <http://www.gadm.org> [Accessed: 10th March 2015]
- Galin VY, Volodin EM, Smyshliaev SP (2003) Atmospheric general circulation model of INM RAS with ozone dynamics. *Russ Meteorol Hydrol* 5:13–22
- GFDL-GAMDT, GFDL Global Atmospheric Model Development Team (2004) The new GFDL global atmosphere and land model AM2-LM2: evaluation with prescribed SST simulations. *J Clim* 17(24):4641–4673
- GLCF, Global and Land Cover Facility (2015) Earth science data interface [Online] Available from <http://www.landcover.org/data/srtm/> [Accessed: 05th March 2015]
- Gordon C, Cooper C, Senior CA, Banks H and others (2000) The simulation of SST, sea ice extents and ocean heat transports in a version of the Hadley Centre coupled model without flux adjustments. *Clim Dyn* 16(2):147–168
- Gordon HB, Rotstayn LD, McGregor JL, Dix MR, Kowalczyk EA, O’Farrell SP, Waterman LJ, Hirst AC, Wilson SG, Collier MA, Watterson IG (2002) The CSIRO Mk3 climate system model. CSIRO Atmospheric Research, Aspendale
- Hourdin F, Musat I, Bony S, Braconnot P, Codron F, Dufresne JL, Fairhead L, Filiberti MA, Friedlingstein P, Grandpeix JY, Krinner G (2006) The LMDZ4 general circulation model: climate performance and sensitivity to parameterized physics with emphasis on tropical convection. *Clim Dyn* 27(7):787–813
- IPCC (2007) Intergovernmental panel on climate change. In: Parry ML, Canziani O F, Palutikof JP, van der Linden PJ, Hanson CE (Eds.), *Climate change 2007: Impacts, adaptation, and vulnerability. Contribution of working group II to the fourth assessment report of the intergovernmental panel on climate change*, Cambridge University Press, Cambridge, pp. 1–976
- ITS (2016) IBM SPSS statistics 23 Part 3: Regression analysis. Winter 2016, Version 1, Information Technology Services (ITS), California State University, Los Angeles, USA
- K-1 Model Developers (2004) K-1 Coupled Model (MIROC) description. Center for Climate System Research, University of Tokyo
- Kiehl JT, Gent PR (2004) The community climate system model, version 2. *J Clim* 17(19):3666–3682
- Kiehl JT, Hack JJ, Bonan GB, Boville BA, Williamson DL, Rasch PJ (1998) The national center for atmospheric research community climate model: CCM3. *J Climate* 11(6):1131–1149. [https://doi.org/10.1175/1520-0442\(1998\)011<1131:TNCFAR>2.0.CO;2](https://doi.org/10.1175/1520-0442(1998)011<1131:TNCFAR>2.0.CO;2)
- Mao Y, Nijssen B, Lettenmaier DP (2015) Is climate change implicated in the 2013–2014 California drought? A hydrologic perspective. *Geophys Res Lett* 42(8):2805–2813. <https://doi.org/10.1002/2015GL063456>
- Martin GM, Ringer MA, Pope VD, Jones A, Dearden C, Hinton TJ (2006) The physical properties of the atmosphere in the new Hadley Centre global environmental model (HadGEM1). I. Model description and global climatology. *J Clim* 19(7):1274–1301
- McFarlane NA, Boer GJ, Blanchet JP, Lazare M (1992) The Canadian Climate Centre second-generation general circulation model and its equilibrium climate. *J Clim* 5(10):1013–1044
- Mohammed R, Scholz M (2017a) Impact of evapotranspiration formulations at various elevations on the reconnaissance drought index. *Water Resour Manag* 31:531–538. <https://doi.org/10.1007/s11269-016-1546-9>
- Mohammed R, Scholz M (2017b) The reconnaissance drought index: a method for detecting regional arid climatic variability and potential drought risk. *J. Arid Environ* 144(2017):181–191. <https://doi.org/10.1016/j.jaridenv.2017.03.014>
- Mohammed R, Scholz M (2017c) Adaptation strategy to mitigate the impact of climate change on water resources in arid and semi-arid regions: a case study. *Water Resour Manag* 31(11):1–17. <https://doi.org/10.1007/s11269-017-1685-7>
- Mohammed R, Scholz M, Nanekely MA, Mokhtari Y (2017a) Assessment of models predicting anthropogenic interventions and climate variability on surface runoff of the Lower Zab River. *Stoch Env Res Risk A* in press
- Mohammed R, Scholz M, Zounemat-Kermani M (2017b) Temporal hydrologic alterations coupled with climate variability and drought for transboundary river basins. *Water Resour Manag* 31:1489–1502. <https://doi.org/10.1007/s11269-017-1590-0>
- Pope VD, Gallani ML, Rowntree PR, Stratton RA (2000) The impact of new physical parametrizations in the Hadley Centre climate model: HadAM3. *Clim Dyn* 16(2):123–146
- Ringer MA, Martin GM, Greeves CZ, Hinton TJ, James PM, Pope VD, Scaife AA, Stratton RA, Inness PM, Slingo JM, Yang GY (2006) The physical properties of the atmosphere in the new Hadley Centre

- Global Environmental Model (HadGEM1). Part II: aspects of variability and regional climate. *J Clim* 19(7):1302–1326
- Roeckner E, Arpe K, Bengtsson L, Christoph M and others (1996) The atmospheric general circulation model ECHAM-4: model description and simulation of present-day climate. Max-Planck-Institut für Meteorologie, Hamburg, Germany
- Russell GL, Miller JR, Rind D (1995) A coupled atmosphere–ocean model for transient climate change studies. *Atmosphere-Ocean* 33(4):683–730
- Semenov MA, Stratonovitch P (2010) Use of multi-model ensembles from global climate models for assessment of climate change impacts. *Clim Res* 41(1): 1–1):14
- Semenov MA, Pilkington-Bennett S, Calanca P (2013) Validation of ELPIS 1980-2010 baseline scenarios using the observed European Climate Assessment data set. *Clim Res* 57:1–9. <https://doi.org/10.3354/cr01164>
- Tigkas D, Vangelis H, Tsakiris G (2012) Drought and climatic change impact on streamflow in small watersheds. *Sci Total Environ* 440: 33–41. <https://doi.org/10.1016/j.scitotenv.2012.08.035>
- Wang B, Wan H, Ji Z, Zhang X, Yu R, Yu Y, Liu H (2004) Design of a new dynamical core for global atmospheric models based on some efficient numerical methods. *Sci China Ser A Math* 47:4–21